



HAL
open science

On the optimal experimental design for heat and moisture parameter estimation

Julien Berger, Denys Dutykh, Nathan Mendes

► **To cite this version:**

Julien Berger, Denys Dutykh, Nathan Mendes. On the optimal experimental design for heat and moisture parameter estimation. *Experimental Thermal and Fluid Science*, 2017, 81, pp.109-122. 10.1016/j.expthermflusci.2016.10.008 . hal-01334414v2

HAL Id: hal-01334414

<https://hal.science/hal-01334414v2>

Submitted on 11 Oct 2016

HAL is a multi-disciplinary open access archive for the deposit and dissemination of scientific research documents, whether they are published or not. The documents may come from teaching and research institutions in France or abroad, or from public or private research centers.

L'archive ouverte pluridisciplinaire **HAL**, est destinée au dépôt et à la diffusion de documents scientifiques de niveau recherche, publiés ou non, émanant des établissements d'enseignement et de recherche français ou étrangers, des laboratoires publics ou privés.



Distributed under a Creative Commons Attribution - NonCommercial - ShareAlike 4.0 International License

Julien BERGER

Pontifical Catholic University of Paraná, Brazil

Denys DUTYKH

CNRS-LAMA, Université Savoie Mont Blanc, France

Nathan MENDES

Pontifical Catholic University of Paraná, Brazil

ON THE OPTIMAL EXPERIMENTAL
DESIGN FOR HEAT AND MOISTURE
PARAMETER ESTIMATION

LAST MODIFIED: October 11, 2016

ON THE OPTIMAL EXPERIMENTAL DESIGN FOR HEAT AND MOISTURE PARAMETER ESTIMATION

JULIEN BERGER*, DENYS DUTYKH, AND NATHAN MENDES

ABSTRACT. In the context of estimating material properties of porous walls based on in-site measurements and identification method, this paper presents the concept of Optimal Experiment Design (OED). It aims at searching the best experimental conditions in terms of quantity and position of sensors and boundary conditions imposed to the material. These optimal conditions ensure to provide the maximum accuracy of the identification method and thus the estimated parameters. The search of the OED is done by using the FISHER information matrix and a priori knowledge of the parameters. The methodology is applied for two case studies. The first one deals with purely conductive heat transfer. The concept of optimal experiment design is detailed and verified with 100 inverse problems for different experiment designs. The second case study combines a strong coupling between heat and moisture transfer through a porous building material. The methodology presented is based on a scientific formalism for efficient planning of experimental work that can be extended to the optimal design of experiments related to other problems in thermal and fluid sciences.

Key words and phrases: inverse problem; parameter estimation; Optimal Experiment Design (OED); heat and moisture transfer; sensitivity functions

MSC: [2010] 35R30 (primary), 35K05, 80A20, 65M32 (secondary)

PACS: [2010] 44.05.+e (primary), 44.10.+i, 02.60.Cb, 02.70.Bf (secondary)

Key words and phrases. inverse problem; parameter estimation; Optimal Experiment Design (OED); heat and moisture transfer; sensitivity functions.

* Corresponding author.

CONTENTS

1	Introduction	4
2	Optimal Experiment Design for non-linear heat transfer problem	5
2.1	Physical problem and mathematical formulation	5
2.2	Optimal experiment design	7
2.3	Numerical example	9
	Estimation of one single parameter	10
	Verification of the ODE	11
3	Optimal Experiment Design for a non-linear coupled heat and moisture transfer problem	17
3.1	Physical problem and mathematical formulation	17
3.2	Optimal experiment design	19
3.3	Numerical example	19
	Estimation of one single parameter	20
	Estimation of several parameters	21
4	Conclusions	24
	Acknowledgments	28
A	Hygrothermal properties	28
	References	28

1. Introduction

Heating or cooling strategies for buildings are commonly based on numerical building physics mathematical models, which can be calibrated using on-site measurements for estimating the properties of the materials constituting the walls, reducing the discrepancies between model predictions and real performance.

Several experimental works at the scale of the wall can be reported from the literature. Instrumented test cells, as ones presented in [8, 9, 13, 14, 18, 22, 25, 27] provide measured dataset as temperature and relative humidity at different points in the wall for given boundary conditions. Some experiments at the scale of the whole-building are described in [7, 17]. These data can be used to estimate the properties (transport and capacity coefficients) of the materials as reported for instance in [19, 29] for heat transfer and in [23, 34] for coupled heat and moisture transfer.

The estimation of the unknown parameters \mathbf{P} , *e.g.* wall thermophysical properties, based on observed data and identification methods is illustrated in Figure 1. Observed data are experimentally obtained. The latter is established by a design defining the boundary and initial conditions of the material, the type of sensors as well as their quantity and location. Thus, the accuracy of the estimated parameters \mathbf{P} strongly depends on the experiment design. The choice of the measurement devices, of the boundary and initial conditions have consequences on the estimation of the parameter. Furthermore, due to the correlation between the parameters, multiple local solutions of the estimation problem exist. Hence, one can address the following questions: what are the best experimental conditions to provide the best conditioning of the identification method? In particular, how many sensors are necessary? Where are their best locations? What boundary and initial conditions should be imposed? Can we really choose them?

These issues deal with searching the Optimal Experiment Design (OED) that enables to identify the parameters \mathbf{P} of a model with a maximum precision. A first objective of the OED is to adjust the conditions of the experiment design in order to maximize the sensitivity of the output field u to parameters \mathbf{P} . A second objective is to find the optimum location and quantity of sensors. The achievement of these objectives enables to determine conditions of the experiments under which the identification of the parameters will have the maximum accuracy.

The search of the OED is based on quantifying the amount of information contained by the observed field u_{exp} . For this, FISHER information matrix is used [1, 2, 10, 11, 15, 26, 31, 32], considering both the model sensitivity, the measurement devices and the parameter correlation. The sensitivity of the output field u with respect to the model parameters \mathbf{P} is calculated, corresponding to the sensitivity of the cost function of the parameter estimation problem. The higher the sensitivity is, the more information is available in the measurement data and the more accurate is the identification of the parameters. Generally speaking, the methodology of searching the OED is important before starting any experiment aiming at solving parameter estimation problems. It allows choosing with a deterministic approach

the conditions of the experiments. Furthermore, it provides information on the accuracy of parameter estimation.

Several works can be reported on the investigation of OED [1–3, 10, 11, 15, 26, 31, 32]. Among them, in [3], the OED is planned as a function of the quantity of sensors and their location, for the estimation of boundary heat flux of non-linear heat transfer. In [15], the OED is searched for the estimation of transport coefficient in convection-diffusion equation. In [20], the OED is analysed as a function of the boundary heat flux for the identification of the radiative properties of the material. In [30], the OED is investigated for chemical reactions using a Bayesian approach. However, the application of OED theory for non-linear heat and moisture transfer with application for the estimation of the properties of a wall is relatively rare.

This article presents the methodology of searching the OED for experiments aiming at solving parameter estimation problems. In the first Section, the concept of OED is detailed and verified for an inverse problem of non-linear heat transfer. The computation of the model sensitivity to the parameter is specified. The OED is sought as a function of the quantity and location of sensors as well as the amplitude and the frequency of the heat flux at the material boundaries. Then the OED for the estimation of hygrothermal properties considering non-linear heat and moisture transfer is investigated. Finally, some main conclusions and perspectives are outlined in the last Section.

2. Optimal Experiment Design for non-linear heat transfer problem

First, the methodology of searching the OED is detailed for a problem of non-linear heat transfer. A brief numerical example is given to illustrate the results.

2.1. Physical problem and mathematical formulation

The physical problem considers an experiment of a one-dimensional transient conduction heat transfer in domains $x \in \Omega = [0, 1]$ and $t \in [0, \tau]$. The initial temperature in the body is supposed uniform. The surface of the boundary $\Gamma_D = \{x = 1\}$ is maintained at the temperature u_D . A time-harmonic heat flux q , of amplitude A and frequency ω , is imposed at the surface of the body denoted by $\Gamma_q \{x = 0\}$. Therefore, the mathematical

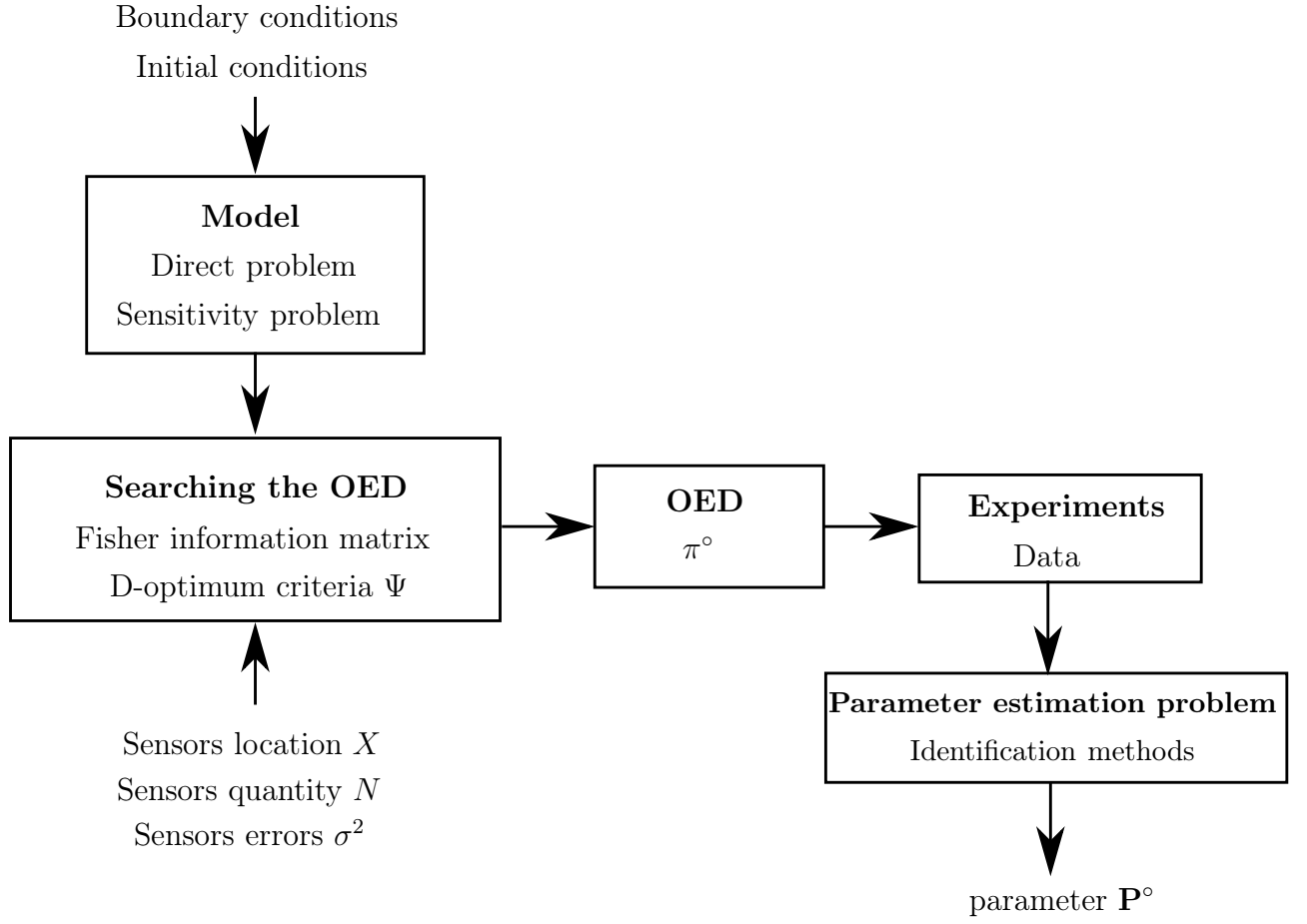


Figure 1. Process of searching the Optimal Experiment Design.

formulation of the heat conduction problem can be written as:

$$c^* \frac{\partial u}{\partial t^*} - \frac{\partial}{\partial x^*} \left(k^*(u) \frac{\partial}{\partial x^*} u \right) = 0 \quad x^* \in \Omega, t^* \in]0, \tau], \quad (2.1a)$$

$$u = u_D \quad x^* \in \Gamma_D, t > 0, \quad (2.1b)$$

$$k^*(u) \frac{\partial u}{\partial x^*} = A^* \sin(2\pi\omega^* t^*) \quad x^* \in \Gamma_q, t > 0, \quad (2.1c)$$

$$u = u_0(x^*) \quad x^* \in \Omega, t^* = 0, \quad (2.1d)$$

$$k^*(u) = (k_0^* + k_1^* u) \quad (2.1e)$$

where the following dimensionless quantities are introduced:

$$\begin{aligned} x^* &= \frac{x}{L}, & u &= \frac{T}{T_{ref}}, & u_D &= \frac{T_D}{T_{ref}}, & u_0 &= \frac{T_0}{T_{ref}}, & k_0^* &= \frac{k_0}{k_r}, \\ k_1^* &= \frac{k_1 T_{ref}}{k_{ref}}, & c^* &= \frac{c}{c_{ref}}, & t_{ref} &= \frac{c_{ref} L^2}{k_{ref}}, & A^* &= \frac{AL}{k_{ref} T_{ref}}, & \omega^* &= \omega t_{ref} \end{aligned}$$

where T is the temperature, c the volumetric heat capacity, k_0 the thermal conductivity and k_1 its dependency on temperature, L the linear dimension of the material, A the intensity and ω the frequency of the flux imposed on surface Γ_q . Subscripts *ref* accounts for a characteristic reference value, D for the Dirichlet boundary conditions, zero (0) for the initial condition of the problem and superscript \star for dimensionless parameters.

The problem given by Eqs. (2.1)(a-e) is a direct problem when all the thermophysical properties, initial and boundary conditions, as well as the body geometry are known. Here, we focus on the inverse problem consisting in estimating one or more parameters of the material properties (as c , k_0 and/or k_1) using the mathematical model Eqs. (2.1)(a-e) and a measured temperature data u_{exp} obtained by N sensors placed in the material at $\mathbf{X} = [x_n], n \in \{1, \dots, N\}$. The M unknown parameters are here denoted as vector $\mathbf{P} = [p_m], m \in \{1, \dots, M\}$. Here, the inverse problems are all non-linear, over-determined solved by considering a least-square single-objective function:

$$J[\mathbf{P}] = \|u_{exp} - \mathfrak{T}(u(x, t, \mathbf{P}))\|^2 \quad (2.2)$$

where u is the solution of the transient heat conduction problem Eqs. (2.1)(a-e). u_{exp} are the data obtained by experiments. They are obtained by N sensors providing a time discrete measure of the field at specified points within the material. \mathfrak{T} is the operator allowing to compare the solution u at the same space-time points where observations u_{exp} are taken. The cost function can be defined in its matrix form, using the ordinary least squares norm, as:

$$J[\mathbf{P}] = [\mathbf{U}_{exp} - \mathbf{U}(\mathbf{P})]^\top [\mathbf{U}_{exp} - \mathbf{U}(\mathbf{P})]$$

where \mathbf{U} is the vector containing the discrete point of the field u for the discrete set of space-time points obtained by the experiments.

For this study, several experiments are distinguished. Ones aim at estimating one parameter: $m = 1$ and $\mathbf{P} = c$, $\mathbf{P} = k_0$ or $\mathbf{P} = k_1$. Others aim at estimating a group of $m = 2$ or $m = 3$ parameters. In this work, the optimal experiment design will be investigated for both cases.

2.2. Optimal experiment design

Efficient computational algorithms for recovering parameters \mathbf{P} have already been proposed. Readers may refer to [21] for a primary overview of different methods. They are based on the minimisation of the cost function $J[\mathbf{P}]$. For this, it is required to equate to

zero the derivatives of $J[\mathbf{P}]$ with respect to each of the unknown parameters p_m . Associated to this necessary condition for the minimisation of $J[\mathbf{P}]$, the scaled dimensionless local sensitivity function [12] is introduced:

$$\Theta_m(x, t) = \frac{\sigma_p}{\sigma_u} \frac{\partial u}{\partial p_m}, \quad \forall m \in \{1, \dots, M\} \quad (2.3)$$

where σ_u is the variance of the error measuring u_{exp} . The parameter scaling factor σ_p equals 1 as we consider that prior information on parameter p_m has low accuracy. It is important to note that all the algorithm have been developed considering the dimensionless problem in order to compare only the order of variation of parameters and observation (and thus avoid units and scales effects).

The sensitivity function Θ_m measures the sensitivity of the estimated field u with respect to change in the parameter p_m [3, 20, 21]. A small value of the magnitude of Θ_m indicates that large changes in p_m yield small changes in u . The estimation of parameter p_m is therefore difficult in such case. When the sensitivity coefficient Θ_m is small, the inverse problem is ill-conditioned. If the sensitivity coefficients are linearly dependent, the inverse problem is also ill-conditioned. Therefore, to get an optimal evaluation of parameters \mathbf{P} , it is desirable to have linearly-independent sensitivity functions Θ_m with large magnitude for all parameters p_m . These conditions ensure the best conditioning of the computational algorithm to solve the inverse problem and thus the better accuracy of the estimated parameter.

It is possible to define the experimental design in order to reach these conditions. The issue is to find the optimal quantity of sensors N° , their optimal location \mathbf{X}° , the optimal amplitude A° and the optimal frequency ω° of the flux imposed at the surface Γ_q . To search this optimal experiment design, we introduce the following measurement plan:

$$\pi = \{N, \mathbf{X}, A, \omega\} \quad (2.4)$$

In analysis of optimal experiment for estimating the unknown parameter(s) \mathbf{P} , a quality index describing the accuracy of recovering is the D -optimum criterion [1–4, 10, 11, 15, 20, 26, 31, 32]:

$$\Psi = \det [F(\pi)] \quad (2.5)$$

where $F(\pi)$ is the normalized Fisher information matrix [15, 31]:

$$F(\pi) = [\Phi_{ij}], \quad \forall (i, j) \in \{1, \dots, M\}^2 \quad (2.6a)$$

$$\Phi_{ij} = \sum_{n=1}^N \int_0^\tau \Theta_i(x_n, t) \Theta_j(x_n, t) dt \quad (2.6b)$$

The matrix $F(\pi)$ characterises the total sensitivity of the system as a function of measurement plan π Eqs. (2.4). The search of the OED aims at finding a measurement plan π^* for which the objective function Eq. (2.5) reaches the maximum value:

$$\pi^\circ = \{N^\circ, \mathbf{X}^\circ, A^\circ, \omega^\circ\} = \arg \max_{\pi} \Psi \quad (2.7)$$

To solve problem (2.7), a domain of variation Ω_π is considered for the quantity of sensors N , their location \mathbf{X} , the amplitude A and the frequency of the flux. Then, the following steps are done for each value of the measurement plan $\pi = \{N, \mathbf{X}, A, \omega\}$ in domain Ω_π .

The direct problem defined by Eqs. (2.1)(a-e) is computed. In this work, it is solved by using a finite-difference standard discretization. An embedded adaptive in time RUNGE–KUTTA scheme combined with central spatial discretization is used. It is adaptive and embedded to estimate local error with little extra cost.

Given the solution u of the direct problem 2.1(a-e) for a fixed value of the measurement plan, the next step consists in computing $\Theta_m = \frac{\partial u}{\partial p_m}$ by solving the sensitivity problem associated to parameter p_m :

$$c \frac{\partial \Theta_m}{\partial t} - \frac{\partial}{\partial x} \left(k \frac{\partial}{\partial x} \Theta_m \right) = - \frac{\partial c}{\partial p_m} \frac{\partial u}{\partial t} + \frac{\partial u}{\partial x} \frac{\partial}{\partial p_m} \left(\frac{\partial k}{\partial x} \right) + \frac{\partial k}{\partial p_m} \frac{\partial^2 u}{\partial x x} \quad x \in \Omega, t > 0, \quad (2.8a)$$

$$\Theta_m = 0 \quad x \in \Gamma_d, t > 0, \quad (2.8b)$$

$$k \frac{\partial \Theta_m}{\partial x} = \frac{\partial u}{\partial x} \frac{\partial k}{\partial p_m} \quad x \in \Gamma_q, t > 0, \quad (2.8c)$$

$$\Theta_m = 0 \quad x \in \Omega, t = 0, \quad (2.8d)$$

$$k = (k_0 + k_1 u) \quad (2.8e)$$

The sensitivity problem Eqs. (2.8) is also solved using an embedded adaptive in time RUNGE–KUTTA scheme combined with central spatial discretization.

It is important to note that the solution of the direct (2.1) problem and the sensitivity (2.8)(a-e) problem are done for a given parameter \mathbf{P} . The later is chosen with the prior information. The validity of the OED depends on the a priori knowledge. If there is no prior information, the methodology of the OED can be done using an outer loop on the parameter \mathbf{P} sampled using Latin hypercube or HALTON quasi-random samplings for instance.

Then, given the sensitivity coefficients, the FISHER matrix (2.6)(a,b) and the D –optimum criterion (2.5) are calculated.

2.3. Numerical example

Current section illustrates the search of optimum experiment design for problem Eqs. (2.1) considering $u_0 = u_D = 1$. The dimension-less properties of the material are equal to $c^* = 10.9$, $k_0^* = 1$, $k_1^* = 0.12$. The final simulation time of the experiment is fixed to $\tau = 28.3$.

From a physical point of view, the numerical values correspond to a material of length $L_r = 0.1$ m. The thermal properties were chosen from a wood fibre: $c = 3.92 \cdot 10^5$ J/m³/K, $k_0 = 0.118$ W/m/K and $k_1 = 5 \cdot 10^{-4}$ W/m/K². The initial temperature of the material is considered uniform at $T_0 = T_{ref} = 293.15$ K. The temperature at the boundary Γ_D is maintained at $T_D = T_{ref} = 293.15$ K. The characteristic time of the problem is $t_{ref} = 3050$

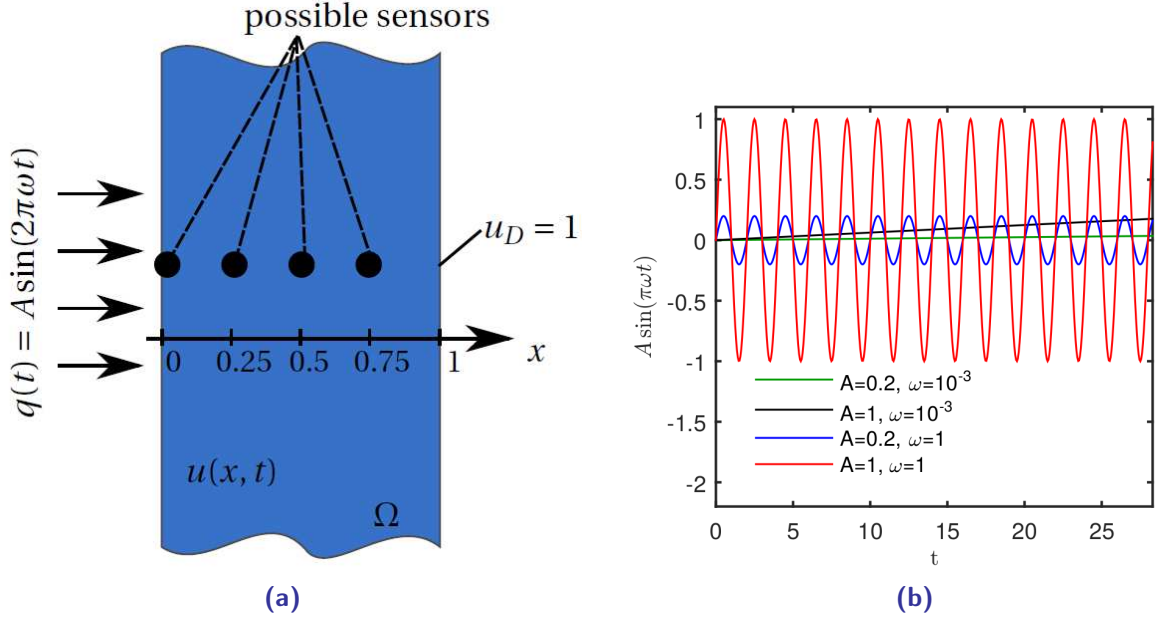


Figure 2. Schematic view of experimental design (a) and the extreme values of the heat flux (b).

s. Thus, the total time of the experiments corresponds to 24 h. A schematic view of the problem is given in Figure 2a.

As mentioned in previous section, the OED is sought as a function of the quantity of sensors N , their location \mathbf{X} , the amplitude A and frequency ω of the flux imposed at the surface Γ_q . For the current numerical application, we consider a maximum of $N = 4$ possible sensors. Their location varies from $\mathbf{X} = [0]$ for $N = 1$ and $\mathbf{X} = [0 \ 0.25 \ 0.5 \ 0.75]$ for $N = 4$ as shown in Figure 2a. The variance of the error measurement equals $\sigma_T = 0.05^\circ\text{C}$. For the amplitude A , 5 values are considered in the interval $[0.2, 1]$ with a regular mesh of 0.2. The minimal value of A corresponds to a physical heat flux of 70 W/m^2 . For the frequency, 30 values have been taken in the interval $[10^{-3}, 1]$. The extreme values of the heat flux are illustrated in Figure 2b.

2.3.1 Estimation of one single parameter

Considering previous description of the numerical example, we first focus on the search of the OED for designing an experiment aiming at estimating one parameter. Thus, \mathbf{P} equals to c , k_0 or k_1 . Figures 3a, 3b and 3c show the variation of the criterion Ψ as a function of the amplitude A and the frequency ω of the heat flux. For each of the three experiments, the criterion is maximum for a low frequency and for a large amplitude as presented in Figure 6. Numerical values of the OED π° are given in Table 1. In terms of physical numerical values, the OED is reached for a heat flux of amplitude 350 W/m^2 and a period of 17.3 h, 60.6h and 53.5h for estimating parameter c , k_0 or k_1 , respectively.

The effect of the numbers of sensors and their positions is given in Figures 4a, 4b and 4c for a fixed amplitude. The criterion increases with the number N of sensor. Adding new sensors yields to a more optimum design. However, it can be noticed the slope of the increase has a small magnitude. For a single sensor $N = 1$, almost 95% of the maximal criterion is reached. Therefore, if the amount of sensors for the experiments is limited, just one sensor located at the boundary receiving the heat flux is available reasonable, enabling to recover one parameter (c , k_0 or k_1). Indeed, the boundary Γ_q is where the sensitivity coefficient of the parameter has the largest magnitude as shown in Figures 5a, 5b and 5c correspondingly.

It can be noticed in Figure 5d that the sensitivity coefficients on the surface $\Gamma_q \equiv \{x = 0\}$ are linearly-independent. Therefore, the inverse problem will not be very sensitive to measurement errors which enables an accurate estimation of the parameters $\mathbf{P} = (c, k_0, k_1)$.

The OED is based on the solution of the direct problem 2.1 and the sensitivity problem 2.8, computed for a given value of the parameter \mathbf{P} . The a-priori knowledge on parameter \mathbf{P} is crucial for the success of the OED. For some applications, there is no prior information on the parameter. For these cases, it is possible to operate an outer loop on the parameter \mathbf{P} sampled in a given domain. For this numerical example, it is considered that there is no prior information on parameters k_0 and k_1 . It is only known their values belong to the domains $[0.1, 0.2]$ W/m/K and $[1 \ 10] \cdot 10^{-4}$ W/m/K². The a priori value of the volumetric heat capacity is still fixed to $c = 3.92 \cdot 10^5$ J/m³/K. A HALTON quasi-random algorithm [16] is then used to generate a sampling of 100 couples of parameters (k_0, k_1) in the domains, as illustrated in Figure 7a. For each couple (k_0, k_1), the methodology described in Section 2.2 is performed to compute the OED. Figure 7b gives the variation of optimal frequency ω° with parameter k_0 and k_1 . The blue points correspond to the results of the OED method for each couple of the discrete sampling. A surface of variation of ω° is then interpolated. It can be noted that the increase of ω° is more important with parameter k_1 .

2.3.2 Verification of the ODE

In order to illustrate the robustness of the ODE, several inverse problems are solved, considering different measurement designs. We consider 30 inverse problems (2.1) of parameter \mathbf{P} associated to the 30 values of the frequency ω in the interval $[10^{-3}, 1]$. For a fixed value of ω , $N_e = 100$ experiments were designed to recover the parameters \mathbf{P} equals to c , k_0 or k_1 and to $\mathbf{P} = (c, k_0, k_1)$. For this purpose, the simulated discrete time observation is obtained by numerical resolution of the direct problem and a uniform sampling with time period $\Delta t = 10$ min. A normal distribution with a standard deviation of $\sigma = 0.01$ was assumed. The inverse problem is solved using Levenberg-Marquardt method [6, 21, 33]. After the solution of the $N_e \times 30$ inverse problems, the empirical mean square error is computed:

$$\text{EMSE}(\omega) = \sqrt{\frac{1}{N_e} (\mathbf{P} - \mathbf{P}^\circ(\omega))^2}, \quad (2.9)$$

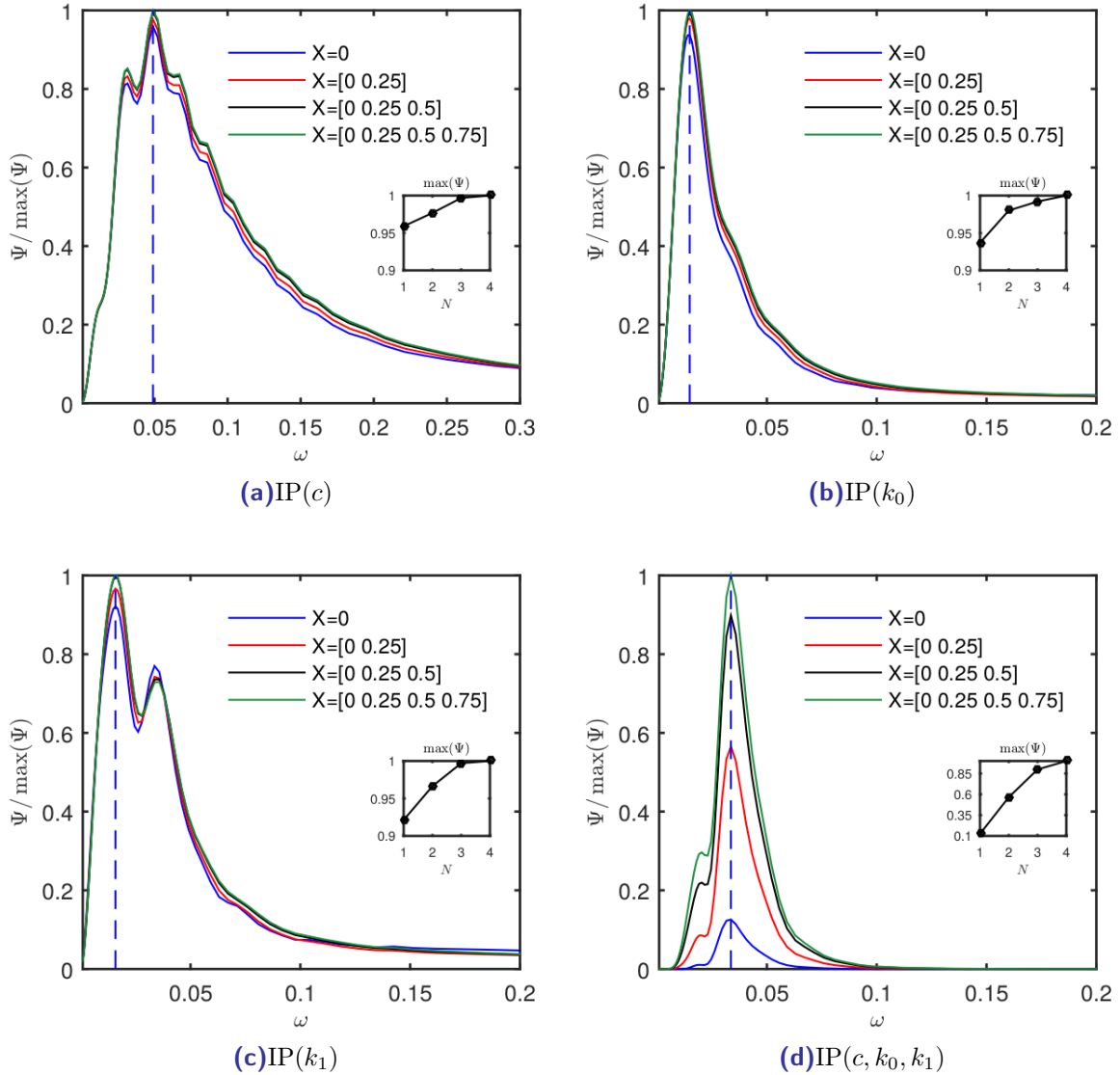


Figure 4. D -optimum criterion Ψ as a function of N , \mathbf{X} and ω for the 4 different experiments ($A = A^\circ = 1$).

In Figure 8a, the variation of the error with the number of the sensors is smooth for the experiments for the estimation of a single parameter. However, for the estimation of several parameters $\mathbf{P} = (c, k_0, k_1)$, the EMSE is below 10^{-2} for three sensors. These results are in accordance with the variation of the criterion Ψ , in Figure 5d. An important variation of the magnitude of Ψ can be observed when passing from $\mathbf{X} = 0$ to $\mathbf{X} = [0 \ 0.25]$.

In Figure 8b, the error is minimised for the optimum experiment design ω° for the four experiments. The estimation of the parameter tends to be inaccurate when the frequency

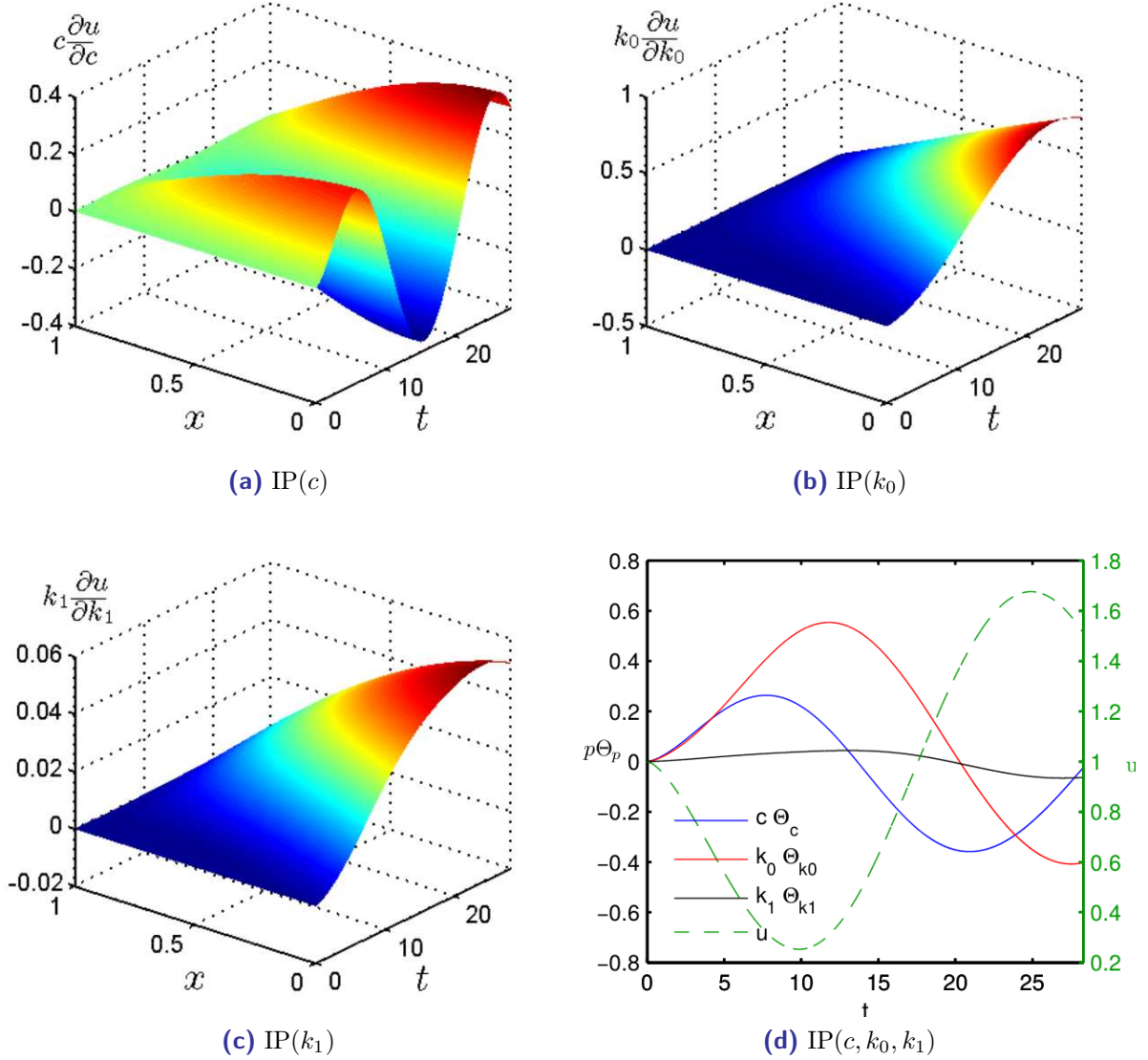


Figure 5. Sensitivity coefficient of parameters for the four different experiments ($N = N^\circ = 1$).

tends to zero, as the heat flux tends to zero and there is almost no solicitation of the material.

For the experiments for the estimation of parameter $\mathbf{P} = c$, the error variation is smooth. As illustrated in Figure 8b, the peak of the criterion Ψ has a large deviation. Therefore, if the frequency ω of the experiments is different from the one of the ODE ω° , the error to estimate the parameter might still be acceptable. For the other experiments, we can notice that the peak of the criterion Ψ has a small deviation in Figures 5b, 5c and 5d.

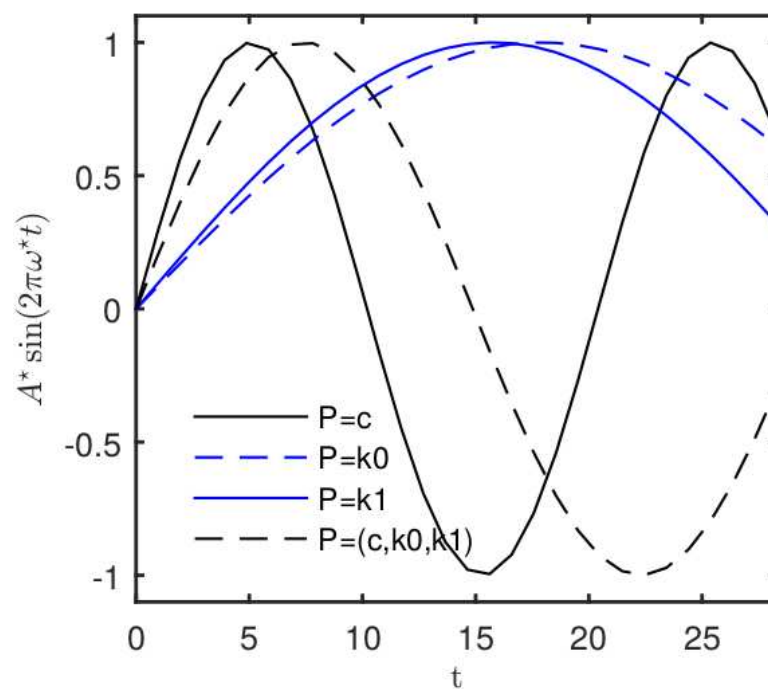


Figure 6. Optimal heat flux for the four different experiments ($N = 1$).

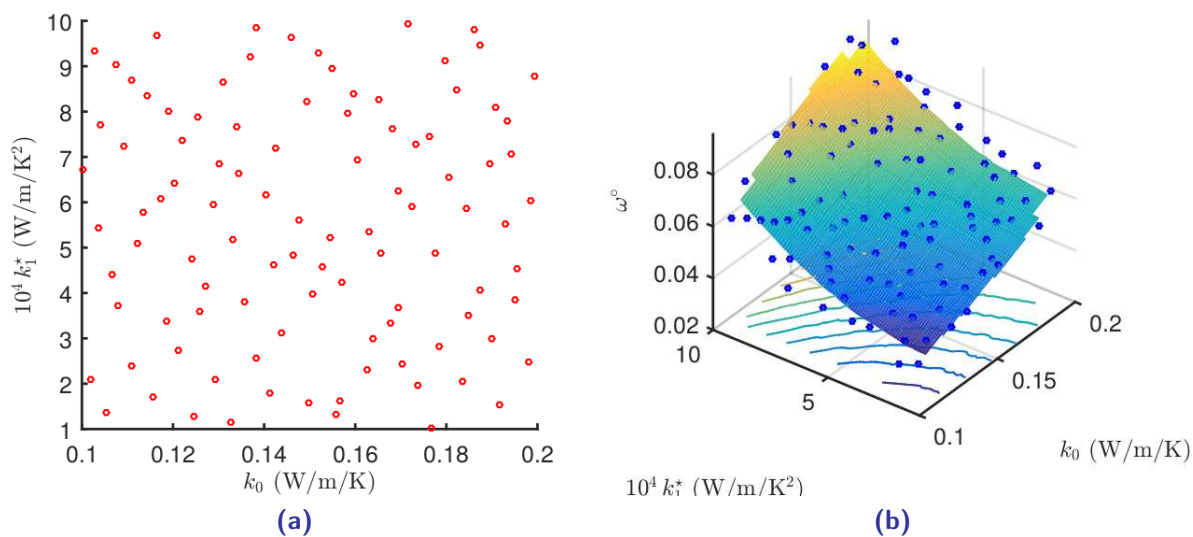


Figure 7. Halton quasi-random sampling of parameters (k_0, k_1) (a) and frequency optimal experiment design ω° (b).

Unknown parameter	max(Ψ)	Optimal experimental design π°					
		A° (-)	A° (W/m ²)	$\frac{1}{\omega^\circ}$ (-)	$\frac{1}{\omega^\circ}$ (h)	N°	X°
$\mathbf{P} = c$	1.4×10^{-2}	1	350	20.4	17.3	1	0
$\mathbf{P} = k_0$	8.6	1	350	71.6	60.6	1	0
$\mathbf{P} = k_1$	3.23	1	350	63.2	53.5	1	0
$\mathbf{P} = (c, k_0, k_1)$	9.1×10^{-3}	1	350	29.7	25.2	3	0

Table 1. Value of the maximum D -optimum criterion for the four different experiments.

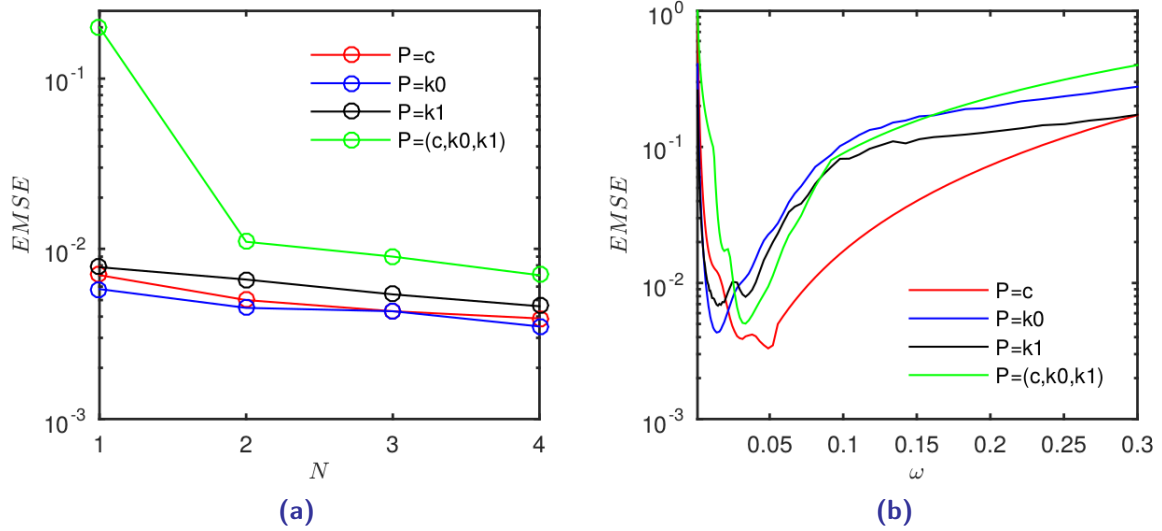


Figure 8. Evolution of the empirical mean square error with the number of sensors (a) and with the frequency ω (b).

The peak of the criterion Ψ has a small deviation in Figures 5b, 5c and 5d. Consequently, the variation of the error in Figure 8b is more important for estimating parameters $\mathbf{P} = k_0$, $\mathbf{P} = k_1$ or $\mathbf{P} = (c, k_0, k_1)$. If the frequency of the experiment design is different from the one of the OED, it implies a loose of accuracy in the estimation of these parameters.

3. Optimal Experiment Design for a non-linear coupled heat and moisture transfer problem

In the previous section, the concept of optimal experiment design was detailed for a non-linear heat transfer problem. It has also been verified for 100 inverse problems for different experiment designs by calculating the error as a function of the frequency and the number of sensors of the measurement plan. In next section, the approach goes further by studying optimal experiment design to estimate transport and storage coefficients of a heat and moisture transfer.

3.1. Physical problem and mathematical formulation

The physical problem concerns a 1-dimensional coupled heat and moisture transfer through a wall based on [5, 23, 24, 28]:

$$c_{10} \frac{\partial T}{\partial t} - \frac{\partial}{\partial x} \left(d_1 \frac{\partial T}{\partial x} \right) - (L_v - c_l T) \frac{\partial}{\partial x} \left(d_2 \frac{\partial P_v}{\partial x} \right) = 0 \quad (3.1a)$$

$$\frac{\partial w}{\partial t} - \frac{\partial}{\partial x} \left(d_2 \frac{\partial P_v}{\partial x} \right) = 0 \quad (3.1b)$$

with w the water content, P_v the vapour pressure, T the temperature, d_2 the vapour permeability, c_{10} the volumetric thermal capacity, d_1 the thermal conductivity, c_l the specific heat capacity of water and L_v the latent heat of evaporation. As this study remains in the hygroscopic range of the material, the liquid transport is not presently taken into account.

The following assumptions are adopted on the properties of the material. The volumetric moisture content is assumed as a first-degree polynomial of the vapour pressure. The vapour permeability and the thermal conductivity are taken as a first-degree polynomial of the volumetric moisture content:

$$\frac{w}{w_0} = c_{20} + \frac{c_{21}}{w_0} P_v \quad (3.2a)$$

$$d_2 = d_{20} + d_{21} \frac{w}{w_0} \quad (3.2b)$$

$$k = d_{10} + d_{11} \frac{w}{w_0} \quad (3.2c)$$

Based on these equations, the experimental set-up considers a material with uniform initial temperature and vapour pressure. At $t > 0$, sinusoidal heat and vapour flux are imposed at boundary $\Gamma_q = \{x = 0\}$, while the temperature and vapour pressure are maintained constant at the other boundary $\Gamma_D = \{x = 1\}$. The unscaled problem can be

formulated as:

$$c_{10}^* \frac{\partial u}{\partial t^*} - \frac{\partial}{\partial x^*} \left(d_1^* \frac{\partial u}{\partial x^*} \right) - (\text{Ko}_1 - \text{Ko}_2) \text{Lu} \frac{\partial}{\partial x^*} \left(d_2^* \frac{\partial v}{\partial x^*} \right) = 0 \quad x^* \in \Omega, t^* \in]0, \tau] \quad (3.3a)$$

$$c_{21}^* \frac{\partial v}{\partial t^*} - \text{Lu} \frac{\partial}{\partial x^*} \left(d_2^* \frac{\partial v}{\partial x^*} \right) = 0 \quad x^* \in \Omega, t^* \in]0, \tau] \quad (3.3b)$$

$$- d_1^* \frac{\partial u}{\partial x^*} = A_1^* \sin(2\pi\omega_1^* t^*) \quad x^* \in \Gamma_q, t^* \in]0, \tau] \quad (3.3c)$$

$$- d_2^* \frac{\partial v}{\partial x^*} = A_2^* \sin(2\pi\omega_2^* t^*) \quad x^* \in \Gamma_q, t^* \in]0, \tau] \quad (3.3d)$$

$$u = u_D, \quad v = v_D \quad x^* \in \Gamma_D, t^* \in]0, \tau] \quad (3.3e)$$

$$u = u_0(x), \quad v = v_0(x) \quad x^* \in \Omega, t^* = 0 \quad (3.3f)$$

$$d_1^* = d_{10}^* + d_{11}^* (c_{20} + c_{21}^* v) \quad (3.3g)$$

$$d_2^* = d_{20}^* + d_{21}^* (c_{20} + c_{21}^* v) \quad (3.3h)$$

with the following dimension-less ratios:

$$\begin{aligned} u &= \frac{T}{T_{ref}} & v &= \frac{P_v}{P_{ref}} & u_0 &= \frac{T_0}{T_{ref}} & v_0 &= \frac{P_{v,0}}{P_{ref}} \\ u_D &= \frac{T_D}{T_{ref}} & v_D &= \frac{P_{v,D}}{P_{ref}} & \text{Ko}_1 &= \frac{L_v c_{2,ref} P_{ref}}{c_{1,ref} T_{ref}} & \text{Ko}_2 &= \frac{c_{L} c_{2,ref} P_{ref}}{c_{1,ref}} \\ \text{Lu} &= \frac{d_{2,ref} c_{1,ref}}{c_{2,ref} d_{1,ref}} & d_{10}^* &= \frac{d_{10}}{d_{1,ref}} & d_{11}^* &= \frac{d_{11}}{d_{1,ref}} & d_{20}^* &= \frac{d_{20}}{d_{2,ref}} \\ d_{21}^* &= \frac{d_{21}}{d_{2,ref}} & c_{10}^* &= \frac{c_{10}}{c_{1,ref}} & c_{21}^* &= \frac{c_{21}}{c_{2,ref}} & c_{2,ref} &= \frac{w_0}{P_{ref}} \\ A_1^* &= \frac{A_1 L}{d_{1,ref} T_{ref}} & A_2^* &= \frac{A_2 L}{d_{2,ref} P_{ref}} & \omega_1^* &= \omega_1 t_{ref} & \omega_2^* &= \omega_2 t_{ref} \\ t^* &= \frac{t}{t_{ref}} & x^* &= \frac{x}{L} & t_{ref} &= \frac{c_{1,ref} L^2}{d_{1,ref}} \end{aligned}$$

where Ko is the KOSOVITICH number, Lu stands for the LUIKOV number, L is the dimension of the material, t_{ref} , the characteristic time of the problem, A and ω the amplitude and intensity of the heat and vapour fluxes. Subscripts *ref* accounts for a reference value,

D for the DIRICHLET boundary conditions, 0 for the initial condition of the problem, 1 for the heat transfer, 2 for the vapour transfer and superscript \star for dimensionless parameters.

3.2. Optimal experiment design

The OED is sought as a function of the quantity of sensors N and their locations X and as a function of the frequencies (ω_1, ω_2) of the heat and vapour fluxes. According to the results of Section 2.3 and to our numerical investigations, a monotonous increase of the sensitivity of the system were observed with the amplitude (A_1, A_2) of the flux. Therefore, these parameters were considered as fixed. Thus, the OED aims at finding the measurement plan π° for which the criterion Eqs. (2.5) reaches a maximum value:

$$\pi^\circ = \{N^\circ, \mathbf{X}^\circ, \omega_1^\circ, \omega_2^\circ\} = \arg \max_{\pi} \Psi \quad (3.4)$$

Parameters L_v, c_L are physical constants given for the problem. Therefore, considering Eqs. (3.3), a number of 7 parameters can be estimated by the resolution of inverse problems: $(c_{10}^\star, d_{10}^\star, d_{11}^\star, c_{20}^\star, c_{21}^\star, d_{20}^\star, d_{21}^\star)$. One can focus on the definition of an experiment for the estimation of one single parameter or several parameters. It might be noted that parameters $(c_{20}^\star, c_{21}^\star, d_{20}^\star, d_{21}^\star)$ can be identified by inverse problems considering field u, v or both (u, v) as observation. The thermal properties $(c_{10}^\star, d_{10}^\star, d_{11}^\star)$ can only be estimated using the observation of u .

All in all, 20 experiments can be defined as:

- i. 15 for the estimation of single parameters among $c_{10}^\star, d_{10}^\star, d_{11}^\star, c_{20}^\star, c_{21}^\star, d_{20}^\star$ or d_{21}^\star ,
- ii. 1 for the estimation of the thermal properties $(c_{10}^\star, d_{10}^\star, d_{11}^\star)$,
- iii. 3 for the estimation of the moisture properties $(c_{20}^\star, c_{21}^\star, d_{20}^\star, d_{21}^\star)$,
- iv. 1 for the estimation of the hygrothermal properties (hg) $(c_{10}^\star, d_{10}^\star, d_{11}^\star, c_{20}^\star, c_{21}^\star, d_{20}^\star, d_{21}^\star)$.

Following notation is adopted: $\text{IP}(p) [u]$ states for an experiment defined for the estimation of parameter p using field u as the observation. The 20 experiments are recalled in Table 2. The same methodology as presented in Section 2 is used. The fifteen sensitivity functions are computed for calculating the criterion (3.4).

3.3. Numerical example

The following numerical values are considered for numerical application. The domain Ω is defined as $\Omega = [0, 1]$, considering the wall thickness of the material as the characteristic length of the problem $L_r = 0.1\text{m}$. The total simulation time of the experiments is $\tau = 6 \times 10^3$, corresponding to a physical simulation of 40 days. The initial and prescribed conditions equal to $u_D = u_0 = 1$ and $v_D = v_0 = 0.5$. The reference temperature and vapour pressure are taken as $T_{ref} = 293.15\text{K}$ and $P_{v,ref} = 2337\text{Pa}$, respectively. The amplitude of the heat and vapour fluxes are $A_1^\star = 1.7 \times 10^{-2}$ and $A_2^\star = 1.7$, equivalent to 600W/m^2 and $1.2 \times 10^{-7}\text{kg/m}^3/\text{s}$.

The dimension-less parameters are:

$$\begin{aligned} \text{Lu} &= 2.5 \times 10^{-4} & \text{Ko}_1 &= 2.1 \times 10^{-1} & \text{Ko}_2 &= 2.5 \times 10^{-2} & d_{10}^* &= 5 \times 10^{-2} & d_{11}^* &= 5 \times 10^{-3} \\ d_{20}^* &= 1 & d_{21}^* &= 0.4 & c_{10}^* &= 1 & c_{20}^* &= 2 & c_{21}^* &= 6 \end{aligned}$$

The properties correspond to a wood fibre material [5, 23]. They are given in its physical dimension in Appendix A.

The OED is sought as a function of the number of the sensors N . It varies from $N = 1$, located at $X = [0]$, to $N = 3$, located at $X = [0 \ 0.2 \ 0.4]$. The variances of the measurement error are $\sigma_T = 0.05^\circ$ and $\sigma_P = 2\text{Pa}$. The OED is also investigated as a function of the frequencies (ω_1^*, ω_2^*) of the flux. For each frequency, 20 values are taken in the interval $[1 \times 10^{-5}; 1.5 \times 10^{-3}]$. The minimal and maximal values correspond to a flux having a physical period of 495 days and 3.3 days, respectively.

As mentioned in Section 2.2, the computation of the solution of the optimal experiment plan is done by successive iterations for the whole grid of the measurement plan $\pi = \{N, X, \omega_1, \omega_2\}$.

3.3.1 Estimation of one single parameter

In the current section, the OED is sought for experiments to estimate one single parameter among c_{10}^* , d_{10}^* , d_{11}^* , c_{20}^* , c_{21}^* , d_{20}^* or d_{21}^* . The results of the ODE are given in Table 2 for the physical values and in Figure 11b for the dimensionless values.

The criterion Ψ varies actively with the frequencies (ω_1^*, ω_2^*) for estimating parameter c_{10}^* , as shown in Figure 9a. The ODE is reached for a period for the heat and vapour flux of 27.2 days.

On the other hand, Figures 9b and 9c illustrate that the criterion varies mostly with the frequency ω_1^* for estimating parameter d_{10}^* and d_{11}^* . The ODE is reached for a period for the heat of 78.1 days. Furthermore, the magnitude of Ψ is really higher than zero, ensuring a good conditioning to solve inverse problems. As observed in the previous section concerning a non-linear heat transfer problem (Section 2.3), the ODE period of the heat flux is shorter for the thermal capacity than for the thermal conductivity.

In Figure 12, the sensitivity functions of parameters d_{10}^* is given for experimental conditions π where Ψ reaches its minimal value and for the ODE conditions (where Ψ reaches its maximal value). In Figure 12a, the magnitude of the sensitivity function is almost 50 times smaller than one for the ODE conditions (Figure 12b). Therefore, the estimation of the parameters might be less accurate for this conditions than the other ones. In Figure 12b, it can be also noticed that the sensitivity function is maximal at the boundary $\Gamma_q = \{x = 0\}$. It emphasizes why the criterion Ψ is maximal for a single sensor settled at this boundary.

For experiments estimating the vapour properties, c_{20}^* , c_{21}^* , d_{20}^* or d_{21}^* , the ODE is not very sensitive to the frequency of the heat flux as reported in Figures 9d, 9e, 9f and 10a. It can be noted that the criterion Ψ is higher when dealing with experiments considering fields (u, v) as observations. The computational algorithm to solve the inverse problem is

better conditioned. The period of the ODE vapour flux is 9.5 and 12.3 days for experiments estimating d_{20}^* and c_{21}^* . Experiments for parameters d_{21}^* and c_{20}^* have the same period of the ODE vapour flux (27.2 days).

It might be recalled that this analysis has been done for a fixed and constant error measurement, equals for the temperature and vapour pressure sensors. Indeed, this hypothesis can be revisited in practical applications. Furthermore, if only one field is available to estimate the vapour properties (u or v), it is required to use the field v as observation and prioritize the accuracy for those sensors. The criterion Φ and the sensitivity is highest for the field v as shown in Figures 13a and 13b.

For all experiments, a single sensor located at $x = 0$ is sufficient to reach more than 95% of the maximum criterion as given in Table 2. The surface receiving the heat and vapour flux is where the sensitivity of the parameters is the higher as illustrated in Figures 13a and 13b for the parameter c_{21} .

3.3.2 Estimation of several parameters

The optimal experiment design is now sought for experiments to estimate several parameters: the thermophysical properties (c_{10}^* , d_{10}^* , d_{11}^*), the moisture properties (c_{20}^* , c_{21}^* , d_{20}^* , d_{21}^*) and the hygrothermal (hg) coefficients (c_{10}^* , d_{10}^* , d_{11}^* , c_{20}^* , c_{21}^* , d_{20}^* , d_{21}^*). Five experiments are considered for the estimation of these parameters as reported in Table 2.

For the estimation of the hygrothermal properties, Figure 10b shows that the criterion Ψ varies mostly with frequency ω_1^* . The criterion is very close to zero (an order of $\mathcal{O}(10^{-9})$). The computational algorithm for the solution of the inverse problem might be ill conditioned. The results of the inverse problem might not be accurate. A way to circumvent the problem is to increase the precision of the sensors and the amplitude of the heat and vapour fluxes.

According to Table 2, the moisture properties might be estimated using both fields (u , v). If it is not possible, the field v would give a more accurate estimation than field u . The criterion varies mostly with the frequency ω_1^* of the heat flux, Figure 10c. The ODE is reached for a period of 35.4 and 16 days for the heat and vapour fluxes, respectively.

For the thermal properties, the criterion varies with both heat and vapour flux frequencies, as reported in Figure 10d. A period of 16 days for both fluxes yields the ODE.

The variation of the criterion with the quantity of sensors is given in Figure 14. As expected, the criterion increases with the number of sensors for all experiments. For the estimation of the hygrothermal properties, the ODE is achieved for 3 sensors. As the vapour properties might be estimated using both fields (u , v), the use of two sensors, located at $x = 0$ and $x = 0.2\text{m}$, for each field, is a reasonable choice that enables to reach more than 95% of the criterion Ψ . In the case, for any reasons, the measurement of both fields is not possible, three sensors measuring the field v are required for the ODE. For the thermal properties, the use of only two sensors is reasonable, as 95% of the maximum criterion is reached. These results are synthesised in Table 2.

<i>Unknown parameter</i>	$\max \{ \Psi \}$	<i>Optimal experimental design π^*</i>		
		$\frac{2\pi}{\omega_1^\circ}$ (days)	$\frac{2\pi}{\omega_2^\circ}$ (days)	N°
IP(c_{10})[u]	6.03	27.2	27.2	1
IP(d_{10})[u]	288	78.1	20.9	1
IP(d_{11})[u]	181	78.1	101.7	1
IP(d_{20})[u]	0.53	7.3	7.3	1
IP(d_{20})[v]	0.99	60	9.5	1
IP(d_{20})[u, v]	1.53	9.5	9.5	1
IP(d_{21})[u]	133	78.1	27.2	1
IP(d_{21})[v]	140	9.5	27.2	1
IP(d_{21})[u, v]	276	78.1	27.2	1
IP(c_{20})[u]	0.02	20.9	20.9	1
IP(c_{20})[v]	0.03	9.5	27.2	1
IP(c_{20})[u, v]	0.05	27.2	27.2	1
IP(c_{21})[u]	0.004	35.4	20.9	1
IP(c_{21})[v]	0.014	78.1	12.3	1
IP(c_{21})[u, v]	0.017	78.1	12.3	1
IP(hg)[u, v]	4.5×10^{-9}	27.2	12.3	3
IP($c_{20}, c_{21}, d_{20}, d_{21}$)[u]	0.001	60.0	20.9	3
IP($c_{20}, c_{21}, d_{20}, d_{21}$)[v]	0.15	12.3	27.2	3
IP($c_{20}, c_{21}, d_{20}, d_{21}$)[u, v]	0.2	35.4	16	2
IP(c_{10}, d_{10}, d_{11})[u]	137	16	16	2

Table 2. Value of the maximum D -optimum criterion for each experiments.

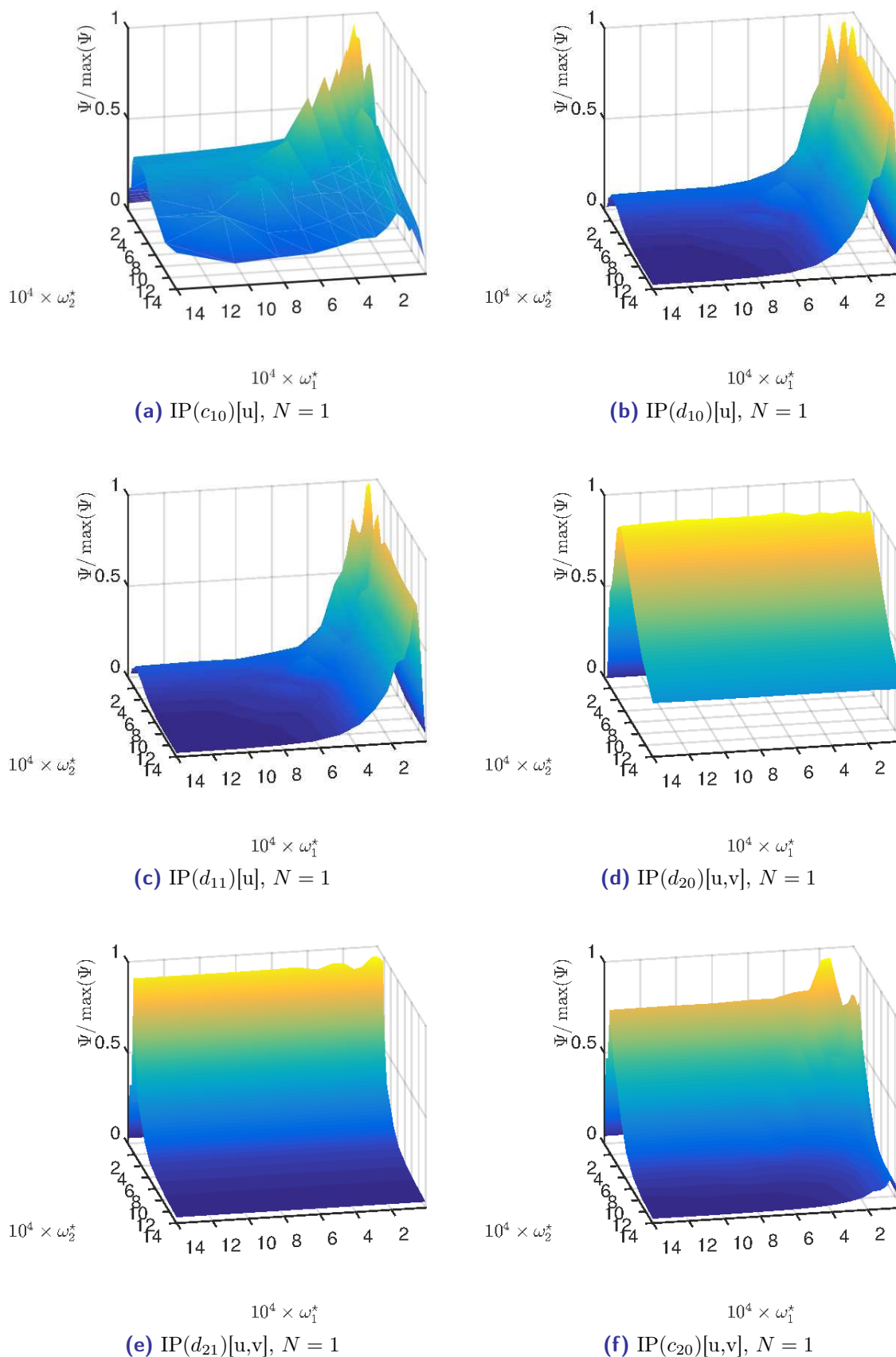


Figure 9. D -optimum criterion Ψ as a function of the frequencies (ω_1, ω_2) .

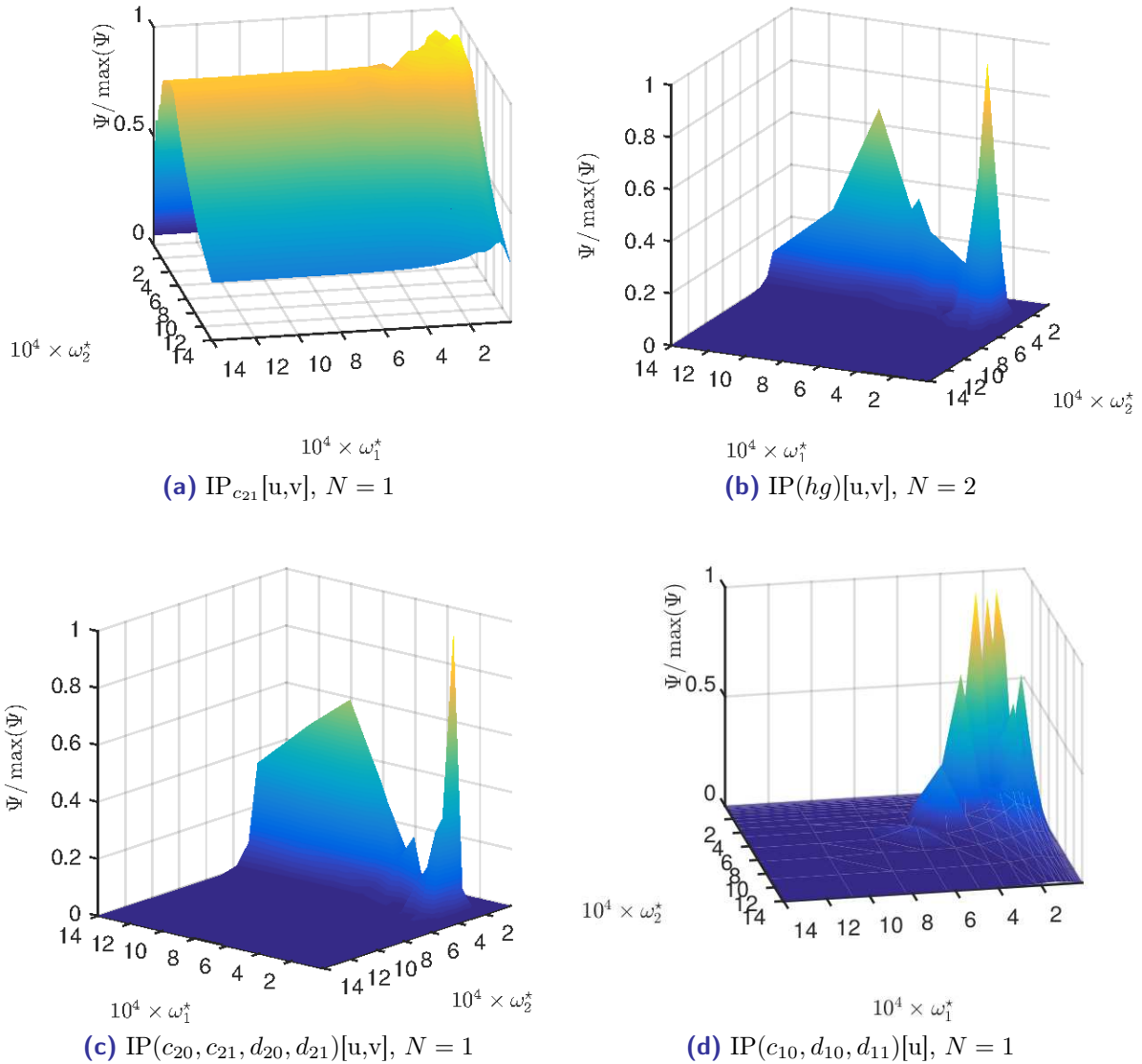


Figure 10. *D*-optimum criterion Ψ as a function of the frequencies (ω_1, ω_2) .

4. Conclusions

In the context of estimating material properties, using in-site measurements of wall in test cells or real buildings combined with identification methods, this study explored the concept of optimal experiment design (OED). It aimed at searching the best experimental conditions in terms of quantity and location of sensors and flux imposed to the material. These conditions ensure to provide the best accuracy of the identification method and thus

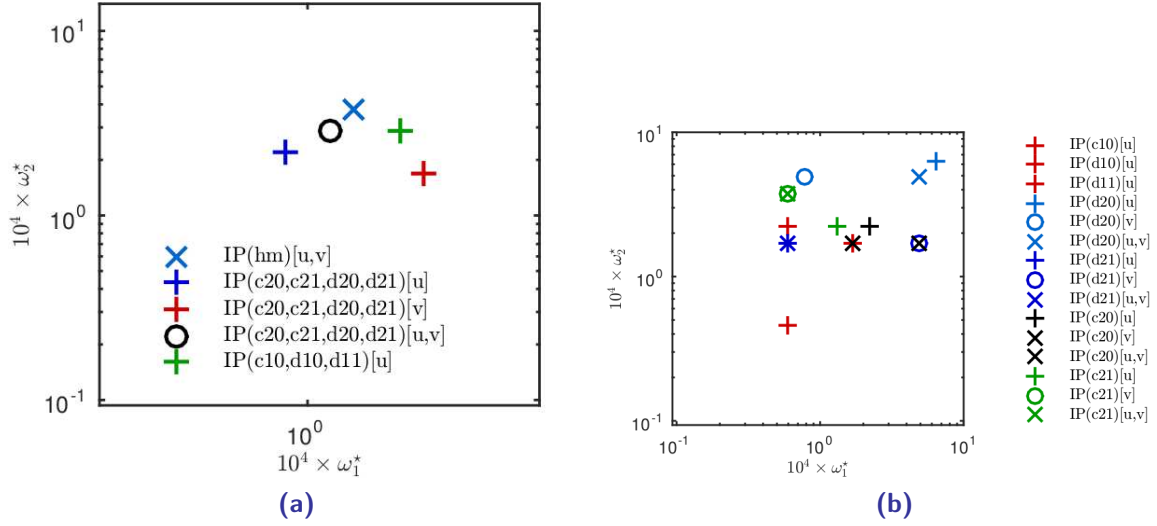


Figure 11. Frequencies ($\omega_1^{*\circ}$, $\omega_2^{*\circ}$) of the ODE.

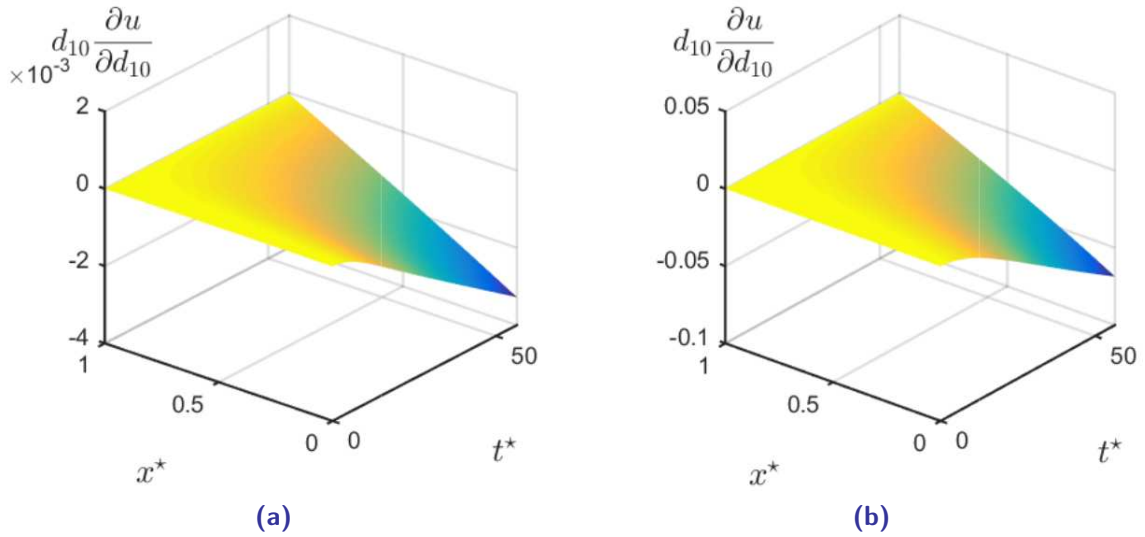


Figure 12. Sensitivity coefficient of parameter k_0 for experimental conditions π where Ψ reaches its minimal value (a) ($\frac{2\pi}{\omega_1} = 3.3$ days, $\frac{2\pi}{\omega_2} = 495$ days, $N = 3$) and for the ODE conditions (b) ($\frac{2\pi}{\omega_1^\circ} = 78.1$ days, $\frac{2\pi}{\omega_2^\circ} = 20.9$ days, $N^\circ = 1$).

the estimated parameter. The search of the OED was done using the FISHER information matrix, quantifying the amount of information contained in the observed field.

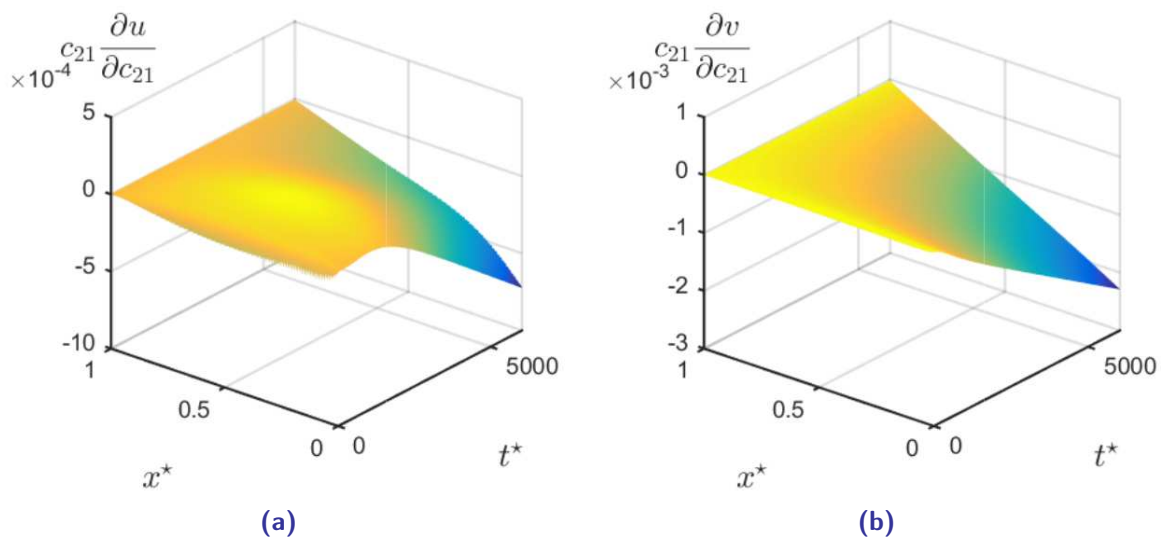


Figure 13. Sensitivity coefficient of parameter c_{21} for the ODE conditions of $IP(c_{21})[u, v]$.

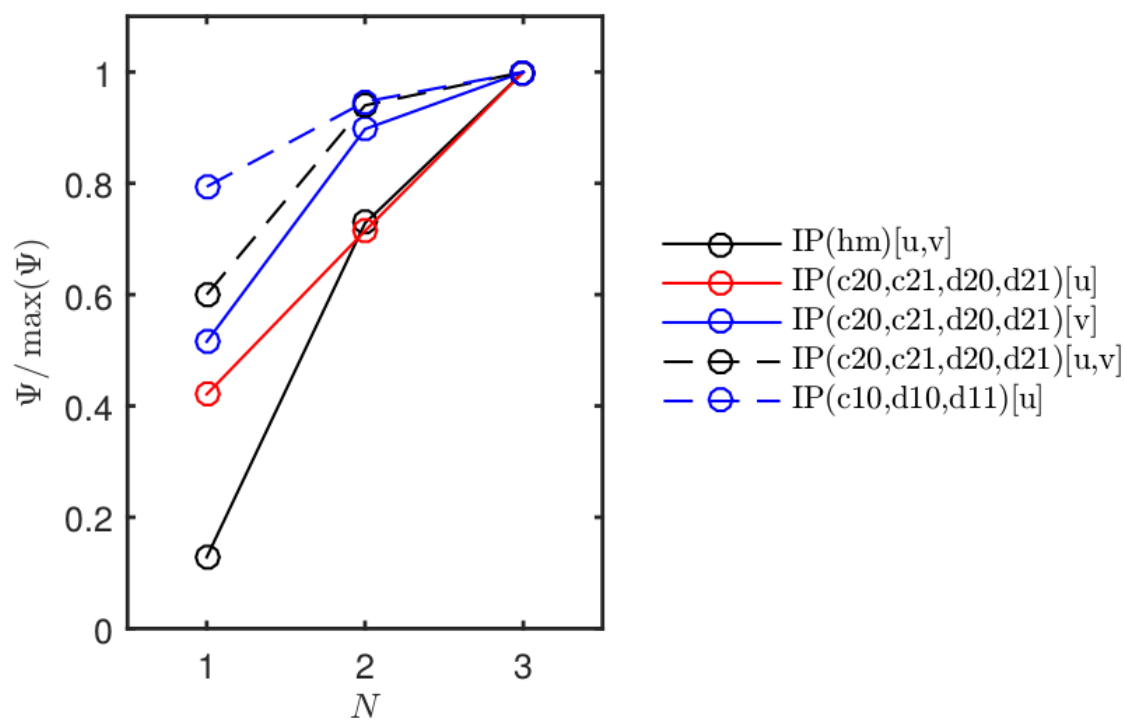


Figure 14. D -optimum criterion Ψ as a function of the quantity of sensors N .

Two cases were illustrated. The first one dealt with an inverse problem of non-linear heat transfer to estimate the thermal properties (storage and transport coefficients), considering a uniform initial temperature field and, as boundary conditions, a fixed prescribed temperature on one side and a sinusoidal heat flux on the other one, for 24 hours. The ODE yields in using one single temperature sensor located at the surface receiving the flux. The flux should have an intensity of 350 W/m^2 and experiment periods of 17 h, 61 h, 54 h and 25 h for the estimation of thermal capacity, thermal conductivity, temperature dependent conductivity and all parameters, respectively. For this case study, the concept of optimal experiment was verified by solving 100 inverse problems for different experiment designs and calculating the error as a function of the frequency and the number of sensors of the measurement plan. It has been demonstrated that the accuracy of the parameter is higher when parameters are recovered with measurements carried out via ODE.

The second application concerned experiments for inverse problems of a coupled non-linear heat and moisture transfer problem to estimate the hygrothermal properties of the material. The experiment is similar to the first case study. Uniform initial distribution of temperature and vapour pressure fields were considered, submitted to harmonic heat and vapour fluxes at one side and prescribed temperature and vapour pressure values at the other one. The experiment was done for a period of 40 days. The achievement of the ODE was explored for different experiments, aiming at estimating one or several parameters. As the equation considered are weakly coupled, the thermal properties can only be determined using the temperature. The accuracy of the identification method does not depend on the vapour flux. For the vapour properties, results have shown that the estimation will be more accurate using the temperature and vapour pressure as observations. Furthermore, the accuracy actively depends on the period of the vapour flux. Single sensor has to be located at the side where the flux is imposed. For experiments to estimate all the hygrothermal properties, two sensors are enough to improve the accuracy.

This contribution explored the concept of optimal experiment design for application in building physics for estimating the hygrothermal properties of construction materials. The methodology of searching the ODE is important before starting any experiment aiming at solving parameter estimation problems. With a priori values of the unknown parameters, the sensitivity functions and the optimum criterion can be computed. Results allow choosing by means of deterministic approach the conditions of the experiments. A good design of experiments avoids installing unnecessary sensors. In the case of coupled phenomena, as the combined heat and moisture transfer problem, considering sensor accuracies, ODE enables to choose and select the field that must be monitored. It also improves the accuracy of the solution of the estimation problem.

Further work is expected to be carried out with different design strategies (ODE and others), estimating properties using real observations.

<i>Properties</i>	<i>Value</i>
d_{10} (W/m/K)	0.5
d_{11} (W/m/K/Pa)	0.05
d_{20} (s)	2.5×10^{-11}
d_{21} (s/Pa)	1×10^{-11}
c_{11} (J/m ³ /K)	4×10^5
c_{20} (-)	2
c_{21} (s ² /m ²)	2.5×10^{-2}
<i>Physical constant</i>	<i>Value</i>
L_v (J/kg)	2.5×10^6
c_L (J/kg)	1000

Table 3. *Hygrothermal properties of the material.*

Acknowledgments

The authors acknowledge the Brazilian Agencies CAPES of the Ministry of Education and the CNPQ of the Ministry of Science, Technology and Innovation for the financial support. Dr. DUTYKH also acknowledges the hospitality of PUCPR during his visit in April 2016.

A. Hygrothermal properties

The hygrothermal properties of the material used in Section 3.3 are given in Table 3.

References

- [1] O. M. Alifanov, E. A. Artioukhine, and S. V. Rumyantsev. *Extreme Methods for Solving Ill-Posed Problems with Applications to Inverse Heat Transfer Problems*. Begellhouse, New York, 1995. 4, 5, 8
- [2] M. L. Anderson, W. Bangerth, and G. F. Carey. Analysis of parameter sensitivity and experimental design for a class of nonlinear partial differential equations. *Int. J. Num. Meth. Fluids*, 48(6):583–605, jun 2005. 4

- [3] E. A. Artyukhin and S. A. Budnik. Optimal planning of measurements in numerical experiment determination of the characteristics of a heat flux. *Journal of Engineering Physics*, 49(6):1453–1458, dec 1985. [5](#), [8](#)
- [4] J. V. Beck and K. J. Arnold. *Parameter Estimation in Engineering and Science*. John Wiley & Sons, Inc., New York, 1977. [8](#)
- [5] J. Berger, M. Chhay, S. Guernouti, and M. Woloszyn. Proper generalized decomposition for solving coupled heat and moisture transfer. *Journal of Building Performance Simulation*, 8(5):295–311, sep 2015. [17](#), [20](#)
- [6] J. Berger, S. Gasparin, M. Chhay, and N. Mendes. Estimation of temperature-dependent thermal conductivity using proper generalised decomposition for building energy management. *Journal of Building Physics*, jun 2016. [11](#)
- [7] R. Cantin, J. Burgholzer, G. Guarracino, B. Moujalled, S. Tamelikecht, and B. Royet. Field assessment of thermal behaviour of historical dwellings in France. *Building and Environment*, 45(2):473–484, feb 2010. [4](#)
- [8] T. Colinart, D. Lelievre, and P. Glouannec. Experimental and numerical analysis of the transient hygrothermal behavior of multilayered hemp concrete wall. *Energy and Buildings*, 112:1–11, jan 2016. [4](#)
- [9] T. Z. Desta, J. Langmans, and S. Roels. Experimental data set for validation of heat, air and moisture transport models of building envelopes. *Building and Environment*, 46(5):1038–1046, may 2011. [4](#)
- [10] A. F. Emery and A. V. Nenarokomov. Optimal experiment design. *Measurement Science and Technology*, 9(6):864–876, jun 1998. [4](#), [5](#), [8](#)
- [11] T. D. Fadale, A. V. Nenarokomov, and A. F. Emery. Two Approaches to Optimal Sensor Locations. *Journal of Heat Transfer*, 117(2):373, 1995. [4](#), [5](#), [8](#)
- [12] S. Finsterle. Practical notes on local data-worth analysis. *Water Resources Research*, 51(12):9904–9924, dec 2015. [8](#)
- [13] C. James, C. J. Simonson, P. Talukdar, and S. Roels. Numerical and experimental data set for benchmarking hygroscopic buffering models. *Int. J. Heat Mass Transfer*, 53(19-20):3638–3654, sep 2010. [4](#)
- [14] T. Kalamees and J. Vinha. Hygrothermal calculations and laboratory tests on timber-framed wall structures. *Building and Environment*, 38(5):689–697, may 2003. [4](#)
- [15] M. Karalashvili, W. Marquardt, and A. Mhamdi. Optimal experimental design for identification of transport coefficient models in convection-diffusion equations. *Computers & Chemical Engineering*, 80:101–113, sep 2015. [4](#), [5](#), [8](#)
- [16] L. Kocis and W. J. Whiten. Computational investigations of low-discrepancy sequences. *ACM Transactions on Mathematical Software*, 23(2):266–294, jun 1997. [11](#)
- [17] M. Labat, M. Woloszyn, G. Garnier, and J. J. Roux. Dynamic coupling between vapour and heat transfer in wall assemblies: Analysis of measurements achieved under real climate. *Building and Environment*, 87:129–141, may 2015. [4](#)
- [18] D. Lelievre, T. Colinart, and P. Glouannec. Hygrothermal behavior of bio-based building materials including hysteresis effects: Experimental and numerical analyses. *Energy and Buildings*, 84:617–627, dec 2014. [4](#)
- [19] A. Nassiopoulos and F. Bourquin. On-Site Building Walls Characterization. *Numerical Heat Transfer, Part A: Applications*, 63(3):179–200, jan 2013. [4](#)

- [20] A. V. Nenarokomov and D. V. Titov. Optimal experiment design to estimate the radiative properties of materials. *Journal of Quantitative Spectroscopy and Radiative Transfer*, 93(1-3):313–323, jun 2005. 5, 8
- [21] M. N. Ozisik and H. R. B. Orlande. *Inverse Heat Transfer: Fundamentals and Applications*. CRC Press, New York, 2000. 7, 8, 11
- [22] H. Rafidiarison, R. Rémond, and E. Mougel. Dataset for validating 1-D heat and mass transfer models within building walls with hygroscopic materials. *Building and Environment*, 89:356–368, jul 2015. 4
- [23] S. Rouchier, M. Woloszyn, Y. Kedowide, and T. Béjat. Identification of the hygrothermal properties of a building envelope material by the covariance matrix adaptation evolution strategy. *Journal of Building Performance Simulation*, 9(1):101–114, jan 2016. 4, 17, 20
- [24] H.-J. Steeman, M. Van Belleghem, A. Janssens, and M. De Paepe. Coupled simulation of heat and moisture transport in air and porous materials for the assessment of moisture related damage. *Building and Environment*, 44(10):2176–2184, oct 2009. 17
- [25] E. Stéphan, R. Cantin, A. Caucheteux, S. Tasca-Guernouti, and P. Michel. Experimental assessment of thermal inertia in insulated and non-insulated old limestone buildings. *Building and Environment*, 80:241–248, oct 2014. 4
- [26] N.-Z. Sun. Structure reduction and robust experimental design for distributed parameter identification. *Inverse Problems*, 21(2):739–758, apr 2005. 4, 5, 8
- [27] P. Talukdar, S. O. Olutmayin, O. F. Osanyintola, and C. J. Simonson. An experimental data set for benchmarking 1-D, transient heat and moisture transfer models of hygroscopic building materials. Part I: Experimental facility and material property data. *Int. J. Heat Mass Transfer*, 50(23-24):4527–4539, nov 2007. 4
- [28] F. Tariku, K. Kumaran, and P. Fazio. Transient model for coupled heat, air and moisture transfer through multilayered porous media. *Int. J. Heat Mass Transfer*, 53(15-16):3035–3044, jul 2010. 17
- [29] S. Tasca-Guernouti, B. Flament, L. Bourru, J. Burgholzer, A. Kindinis, R. Cantin, B. Moujalled, G. Guarracino, and T. Marchal. Experimental Method to determine Thermal Conductivity, and Capacity Values in Traditional Buildings. In *VI Mediterranean Congress of Climatization*, Madrid, Spain, 2011. 4
- [30] G. Terejanu, R. R. Upadhyay, and K. Miki. Bayesian experimental design for the active nitridation of graphite by atomic nitrogen. *Experimental Thermal and Fluid Science*, 36:178–193, jan 2012. 5
- [31] D. Ucinski. *Optimal Measurement Methods for Distributed Parameter System Identification*. 2004. 4, 5, 8
- [32] A. Vande Wouwer, N. Point, S. Porteman, and M. Remy. An approach to the selection of optimal sensor locations in distributed parameter systems. *Journal of Process Control*, 10(4):291–300, aug 2000. 4, 5, 8
- [33] C.-Y. Yang. Estimation of the temperature-dependent thermal conductivity in inverse heat conduction problems. *Appl. Math. Model.*, 23(6):469–478, jun 1999. 11
- [34] A. Zaknoune, P. Glouannec, and P. Salagnac. Estimation of moisture transport coefficients in porous materials using experimental drying kinetics. *Heat and Mass Transfer*, 48(2):205–215, feb 2012. 4

THERMAL SYSTEMS LABORATORY, MECHANICAL ENGINEERING GRADUATE PROGRAM, PONTIFICAL CATHOLIC UNIVERSITY OF PARANÁ, RUA IMACULADA CONCEIÇÃO, 1155, CEP: 80215-901, CURITIBA – PARANÁ, BRAZIL

E-mail address: Julien.Berger@pucpr.edu.br

URL: https://www.researchgate.net/profile/Julien_Berger3/

LAMA, UMR 5127 CNRS, UNIVERSITÉ SAVOIE MONT BLANC, CAMPUS SCIENTIFIQUE, 73376 LE BOURGET-DU-LAC CEDEX, FRANCE

E-mail address: Denys.Dutykh@univ-savoie.fr

URL: <http://www.denys-dutykh.com/>

THERMAL SYSTEMS LABORATORY, MECHANICAL ENGINEERING GRADUATE PROGRAM, PONTIFICAL CATHOLIC UNIVERSITY OF PARANÁ, RUA IMACULADA CONCEIÇÃO, 1155, CEP: 80215-901, CURITIBA – PARANÁ, BRAZIL

E-mail address: Nathan.Mendes@pucpr.edu.br

URL: https://www.researchgate.net/profile/Nathan_Mendes/